Original Article | Gastrointestinal Imaging

eISSN 2005-8330
https://doi.org/10.3348/kjr.2022.0560
Korean J Radiol 2023;24(3):190-203

Korean Journal of Radiology
KJR

Targetoid Primary Liver Malignancy in Chronic Liver Disease: Prediction of Postoperative Survival Using Preoperative MRI Findings and Clinical Factors

So Hyun Park[1]*, Subin Heo[2]*, Bohyun Kim[3], Jungbok Lee[4], Ho Joong Choi[5], Pil Soo Sung[6], Joon-Il Choi[3]

[1]Department of Radiology, Gil Medical Center, Gachon University College of Medicine, Incheon, Korea; [2]Department of Radiology, Ajou University Hospital, Suwon, Korea; Departments of [3]Radiology, [5]Surgery, and [6]Internal Medicine, Seoul St. Mary's Hospital, College of Medicine, The Catholic University of Korea, Seoul, Korea; [4]Department of Clinical Epidemiology and Biostatistics, Asan Medical Center, University of Ulsan College of Medicine, Seoul, Korea

Objective: We aimed to assess and validate the radiologic and clinical factors that were associated with recurrence and survival after curative surgery for heterogeneous targetoid primary liver malignancies in patients with chronic liver disease and to develop scoring systems for risk stratification.

Materials and Methods: This multicenter retrospective study included 197 consecutive patients with chronic liver disease who had a single targetoid primary liver malignancy (142 hepatocellular carcinomas, 37 cholangiocarcinomas, 17 combined hepatocellular carcinoma-cholangiocarcinomas, and one neuroendocrine carcinoma) identified on preoperative gadoxetic acid-enhanced MRI and subsequently surgically removed between 2010 and 2017. Of these, 120 patients constituted the development cohort, and 77 patients from separate institution served as an external validation cohort. Factors associated with recurrence-free survival (RFS) and overall survival (OS) were identified using a Cox proportional hazards analysis, and risk scores were developed. The discriminatory power of the risk scores in the external validation cohort was evaluated using the Harrell C-index. The Kaplan–Meier curves were used to estimate RFS and OS for the different risk-score groups.

Results: In RFS model 1, which eliminated features exclusively accessible on the hepatobiliary phase (HBP), tumor size of 2–5 cm or > 5 cm, and thin-rim arterial phase hyperenhancement (APHE) were included. In RFS model 2, tumors with a size of > 5 cm, tumor in vein (TIV), and HBP hypointense nodules without APHE were included. The OS model included a tumor size of > 5 cm, thin-rim APHE, TIV, and tumor vascular involvement other than TIV. The risk scores of the models showed good discriminatory performance in the external validation set (C-index, 0.62–0.76). The scoring system categorized the patients into three risk groups: favorable, intermediate, and poor, each with a distinct survival outcome (all log-rank $p < 0.05$).

Conclusion: Risk scores based on rim arterial enhancement pattern, tumor size, HBP findings, and radiologic vascular invasion status may help predict postoperative RFS and OS in patients with targetoid primary liver malignancies.

Keywords: *Hepatocellular carcinoma; Cholangiocarcinoma; Magnetic resonance imaging; Prognosis prediction; Risk score*

INTRODUCTION

Hepatocellular carcinoma (HCC) is the most common type of primary liver malignancy in patients with chronic liver disease [1]. However, in the same population, in addition to typical HCCs with radiologic hallmarks, atypical HCCs and non-HCC primary liver malignancies such as combined HCC and cholangiocarcinoma (CCA) (cHCC-CCA) coexist, hindering diagnosis [1-4]. According to the Liver Imaging Reporting and Data System (LI-RADS), heterogeneous

Received: February 24, 2022 **Revised:** November 2, 2022 **Accepted:** November 23, 2022
*These authors contributed equally to this work.
Corresponding author: Bohyun Kim, MD, PhD, Department of Radiology, Seoul St. Mary's Hospital, College of Medicine, The Catholic University of Korea, 222 Banpo-daero, Seocho-gu, Seoul 06591, Korea.
• E-mail: kbh@catholic.ac.kr

Korean Journal of Radiology
KJR

primary liver malignancies that lack the typical radiologic features of HCC are collectively called "if probably or definitely malignant but not HCC specific" or "LI-RADS M (LR-M)" [2]. Since targetoid appearance is frequent in non-HCC malignancies, the presence of any one targetoid feature is sufficient for LR-M categorization [5].

Targetoid primary liver malignancies require biopsy or further imaging for a conclusive diagnosis [4,6]. Thus, existing studies have focused on radiologic differential diagnosis [7-9]. Definitive surgery is the cure for feasible diseases with preserved liver function [4,6]. Accordingly, preoperative estimation of postoperative outcomes in targetoid primary liver malignancies is likely to influence therapeutic decision-making, potentially modifying the extent of the surgical field or, in patients with HCC, switching to liver transplantation. Studies have shown a poor prognosis for targetoid lesions regardless of the pathologic diagnosis [10-14], but further prognostic stratification within heterogeneous subsets of targetoid primary liver malignancies has rarely been reported. Risk stratification may be possible if other poor prognostic MRI features are added, such as a non-smooth tumor margin [15], corona enhancement [16,17], peritumoral hypointensity on the hepatobiliary phase (HBP) [11,18], and HBP hypointense nodules without arterial phase hyperenhancement (APHE) [19,20].

In this study, we aimed to assess the radiologic and clinical factors associated with recurrence and survival after curative surgery for targetoid primary liver malignancies, as well as establish and validate scoring systems for risk stratification.

MATERIALS AND METHODS

This study was approved by the Institutional Review Boards of the three participating centers. The requirement for informed consent was waived owing to the retrospective study design (IRB No. KC21RIDI0483, GDIRB2021-455, and AJIRB-MED-MDB-22-221).

Study Population

Consecutive adult patients with chronic liver disease who underwent curative surgery for suspicious liver lesions between January 2010 and December 2017 were recruited from three centers. The inclusion criteria were: 1) a single primary liver malignancy confirmed by surgical pathology, and 2) a preoperative gadoxetic acid-enhanced MRI examination within three months of surgery. The exclusion criteria were: 1) prior treatment, including resection, locoregional treatment, or systemic chemotherapy, 2) benign pathology, 3) synchronous or metachronous non-hepatic malignancy, 4) invisible lesions on MRI, and 5) suboptimal MR image quality. Data from centers 1 and 2 (Seoul St. Mary's Hospital and Gil Medical Center) were used to develop the scoring system, and data from center 3 (Ajou University Hospital) was used for the external validation.

Clinicopathologic Data Collection

Clinical and laboratory data, including age at liver surgery, sex, etiology of liver disease, preoperative Child-Pugh score, serum alpha-fetoprotein (AFP) levels, protein induced by vitamin K absence or antagonist II (PIVKA-II), and type of liver surgery, were collected. Pathological data included the histopathologic diagnosis of the lesion, the Edmondson–Steiner grade, a meta-analysis of histological data in viral hepatitis (METAVIR) score, microvascular invasion (MVI), a satellite nodule, and the resection margin status. The diagnosis of cHCC-CCA was made according to the 2010 World Health Organization classification [21].

Liver MRI Protocol

Liver MRI was performed using 1.5T (Magnetom Avanto, Siemens Healthineers; SignaHDxt, GE Healthcare) and 3T scanners (Verio and Skyra, Siemens Healthineers; Discovery 750w, GE Healthcare). The MRI protocol commonly encompasses axial T2-weighted images, diffusion-weighted images (DWI; b = 0, 500, and 800 s/mm^2), and dual gradient-echo images. Late hepatic arterial, portal venous, transitional phase (TP), and HBP images were acquired for a dynamic enhancement study. Detailed MRI parameters and dynamic enhancement study protocols are listed in Supplementary Table 1.

MR Image Analysis

Two abdominal radiologists (with more than nine years of experience in liver MRI) prescreened the MRI examinations to select targetoid liver lesions. After obtaining a consensus on discrepancies, the final targetoid lesions were included in further image analysis (Fig. 1). Three abdominal radiologists with different levels of experience in liver MRI (two with more than nine years and one with more than three years) independently reviewed the anonymized MR images of the development cohort. The reviewers were blinded to the clinicopathologic information of the patients but were aware that the images were of primary

 https://doi.org/10.3348/kjr.2022.0560

liver malignancies in patients with chronic liver disease. Targetoid lesions were defined as the presence of at least one of the following features: rim APHE, peripheral washout, delayed central enhancement, or targetoid appearance on DWI, TP, or HBP [2,22]. Rim APHE was categorized as 1) a smooth, thin rim with a thickness within 25% of the in-plane diameter of the tumor throughout the perimeter, and 2) an irregular, thick rim with a thickness partly or entirely exceeding 25% of the tumor diameter (Figs. 2, 3) [7,23]. Furthermore, corona enhancement, capsule, intralesional fat, peritumoral bile duct dilatation, non-smooth tumor margin, radiologic vascular invasion by a tumor in the vein (TIV), vascular involvement other than TIV (encasement, narrowing, tethering, occlusion, or obliteration) [24], peritumoral hypointensity on HBP, and HBP hypointense nodules without rim or nonrim APHE [25] were assessed. In the presence of both TIV and vascular involvement other than TIV, given the established prognostic impact of TIV, TIV was prioritized but not *vice versa* [26]. Therefore, these two features were mutually exclusive. Only HBP hypointense nodules without APHE with a size of ≥ 3 mm that had not been surgically removed were considered. Detailed definitions of the imaging features are provided in Supplementary Table 2. The MR images of the validation cohort were similarly evaluated by two more experienced readers. A joint review resolved any disagreement in the interpretation.

Outcome Measures

Patient follow-up was performed according to institutional protocols after surgery until April 15, 2021. The follow-up protocols included multiphasic liver CT covering the pelvis or gadoxetic acid-enhanced MRI, serum tumor marker tests, and clinical evaluations every three to six months. For clinical or radiologic suspicion of recurrence, further assessments, including a chest CT, a bone scan, or ^{18}F-fluorodeoxyglucose PET-CT, were conducted. Recurrence-free survival (RFS) was defined as the time from surgery to intra- or extrahepatic recurrence or death [27-29], while overall survival (OS) was defined as the time from surgery to death. Patients with no recurrence or death were excluded at the last follow-up before April 15, 2021.

Statistical Analysis

Continuous variables are expressed as means with standard deviations or medians with interquartile ranges after testing for normality. Categorical variables are expressed as numbers and percentages. A Student's *t* test,

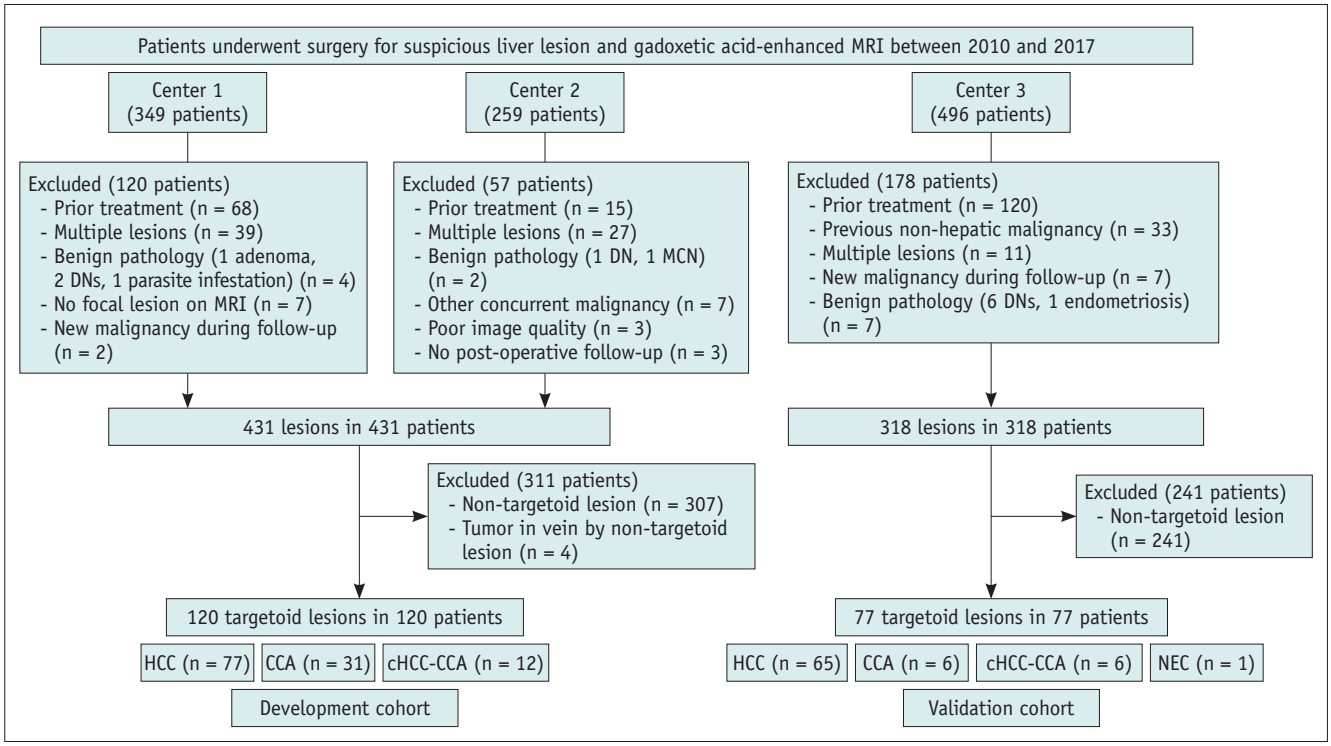

Fig. 1. A flowchart for the selection of the study population. CCA = cholangiocarcinoma, cHCC-CCA = combined HCC and CCA, DN = dysplastic nodule, HCC = hepatocellular carcinoma, MCN = mucinous cystic neoplasm, NEC = neuroendocrine carcinoma

https://doi.org/10.3348/kjr.2022.0560

Korean Journal of Radiology
KJR

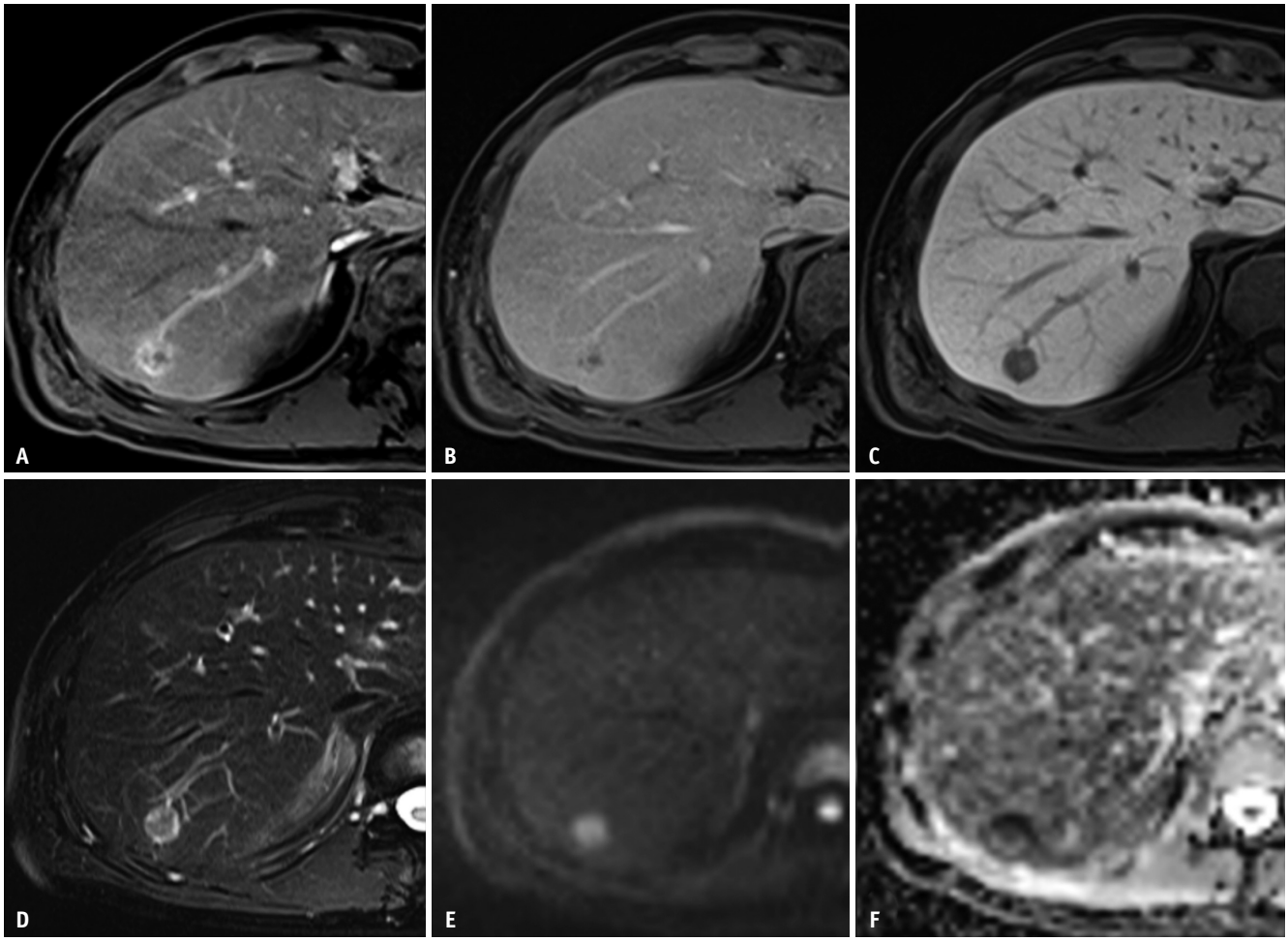

Fig. 2. Preoperative gadoxetic acid-enhanced MR images of a 56-year-old male alcoholic patient with hepatitis.
A-C. There is a 1.4-cm nodule **(A)** with thick arterial rim enhancement in S7 of the liver, with **(B)** portal venous phase washout and **(C)** no peritumoral hypointensity on the hepatobiliary phase. **D-F.** The nodule **(D)** shows a moderately hyperintense T2 signal with **(E, F)** restricted diffusion (b = 800 s/mm^2). The patient belongs to the low-risk group for recurrence. Curative resection found cholangiocarcinoma without microvascular invasion or a satellite nodule. The patient has been disease-free for four years.

Wilcoxon rank-sum test, χ^2 test, or Fisher's exact test was used to compare variables between the development and validation cohorts. The binary cutoff values for AFP and PIVKA-II were calculated using the maximum Youden index value to differentiate between patients who had and did not have a recurrence. Cox proportional hazard analyses with backward elimination identified independent predictors of RFS and OS, with variables with $p < 0.1$ in the univariable analysis transferred for multivariable analysis. Based on multivariable analysis, the risk score was calculated by dividing each correlation coefficient (β) by the smallest β and rounding it to the nearest integer [30]. The sum of the risk scores represented the risk of recurrence or death for each patient. The discriminatory power of the risk score was assessed using Harrell's C-index and the area under the time-dependent receiver operating characteristic area under the curve (AUC) at one, two, and five years. Optimism-corrected C-indices were reported as the primary results [31]. The risk score stratified the risk groups based on the probability of recurrence or death. The Kaplan–Meier method was used to estimate RFS and OS, and differences between groups were compared using the log-rank test. Considering the clinical environment where gadoxetic acid-enhanced MRI is unavailable or HBP imaging is suboptimal, we established two RFS models: model 1, excluding radiologic features accessible only on HBP, and model 2, including all significant factors in univariable analysis. Kappa (κ) statistics were used to evaluate the inter-reader agreement as follows: fair (0.20–0.39), moderate (0.40–0.59), good (0.60–0.79), and excellent (0.80–1.00). All statistical analyses were performed using R software, version 3.6.1 (R Foundation for Statistical Computing), and

 https://doi.org/10.3348/kjr.2022.0560

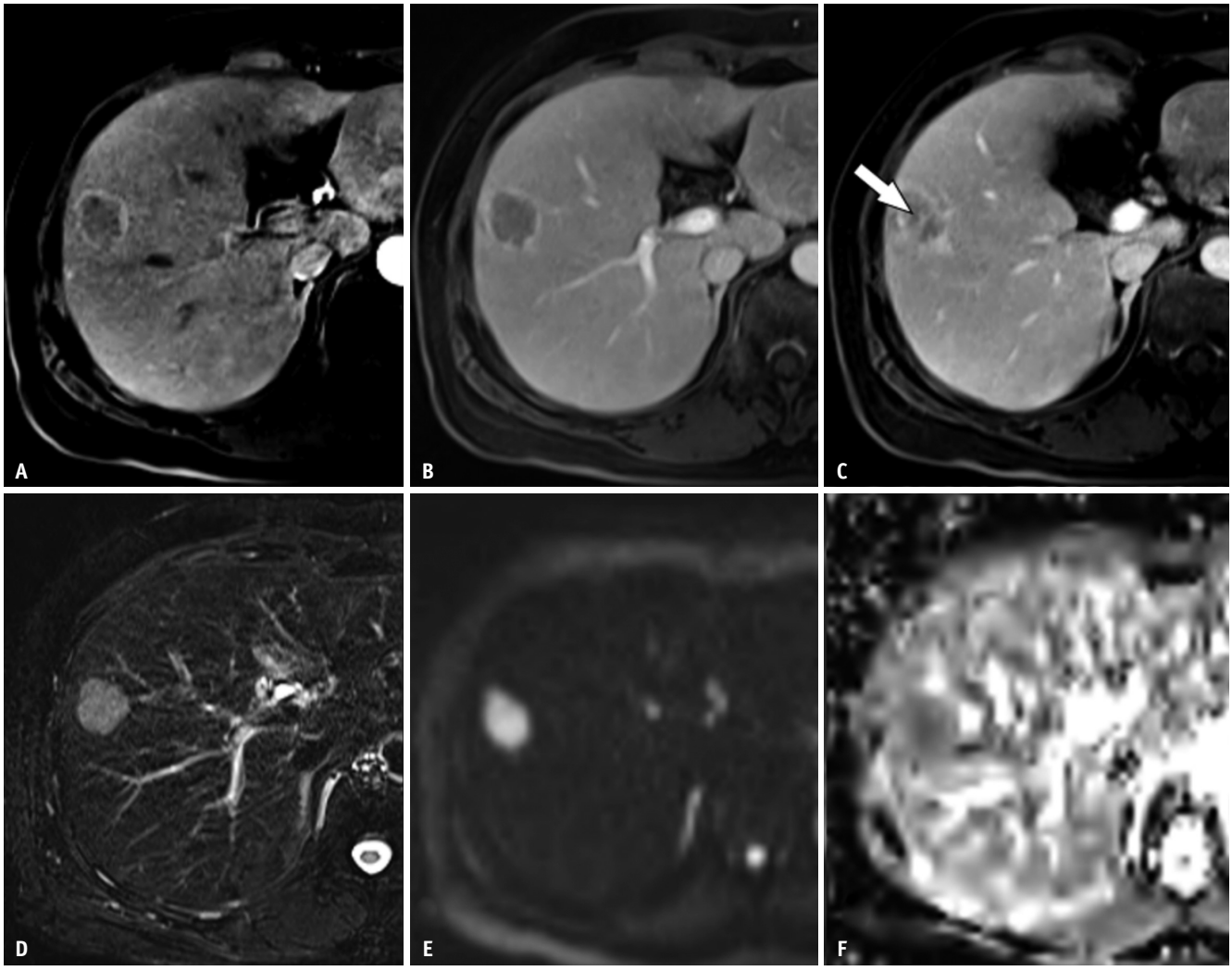

Fig. 3. Preoperative gadoxetic acid-enhanced MR images of a 52-year-old female patient with chronic hepatitis B.
A-C. There is a 2.8-cm nodule **(A)** with thin arterial rim enhancement in S5 of the liver, with **(B)** equivocal portal venous phase washout and **(C)** tumor vascular encasement (arrow). **D-F.** The nodule **(D)** shows a moderately hyperintense T2 signal with **(E, F)** restricted diffusion. The patient belongs to the intermediate-risk group for recurrence. A curative resection found hepatocellular carcinoma with microvascular invasion. Intrahepatic recurrence developed after eight months, and the patient underwent liver transplantation. The patient has been disease-free for seven years since transplantation.

IBM SPSS Statistics for Windows, version 24 (IBM Corp.). A two-tailed $p < 0.05$ indicated statistical significance.

RESULTS

Patient Characteristics

Of the 1104 patients with chronic liver disease who had curative surgery for suspicious liver lesions and preoperative gadoxetic acid-enhanced MRI examinations at three centers, 749 patients with single-treatment-naïve primary liver malignancy were selected based on the inclusion and exclusion criteria. After screening for targetoid liver lesions, 197 patients (120 in the development cohort and 77 in the validation cohort) were included in the study (Fig. 1). Clinicopathological characteristics of the patients are summarized in Table 1. Most patients (80.2%; 95 in the development cohort and 63 in the validation cohort) had chronic hepatitis B viral infection or cirrhosis. Additionally, 102 (51.8%) and 95 (48.2%) patients were imaged using 3T and 1.5T MR units, respectively. Of the excluded benign lesions, parasite infestations (n = 1) had a targetoid appearance.

Gadoxetic Acid-Enhanced MRI Findings of Targetoid Lesions and Inter-Reader Agreement

Table 2 summarizes the MRI findings of the targetoid

https://doi.org/10.3348/kjr.2022.0560

Korean Journal of Radiology
KJR

Table 1. Clinical and Pathologic Characteristics of Study Patients

	Development Cohort (n = 120)	Validation Cohort (n = 77)	*P*
Age, year*	55.4 (9.9)	64.2 (10.1)	< 0.001
Sex (male)	83 (69.2)	71 (92.2)	< 0.001
Etiology of liver disease			> 0.05
Hepatitis B virus	89 (74.2)	61 (79.2)	0.481
Hepatitis C virus	4 (3.3)	3 (3.9)	0.969
Alcohol	4 (3.3)	3 (3.9)	0.969
NAFLD	9 (7.5)	3 (3.9)	0.835
Others	14 (11.7)	7 (9.1)	0.860
Cirrhosis (F4)	50 (41.7)	26 (33.8)	0.268
Hepatitis B virus	44/50 (88.0)	24/26 (92.3)	
Hepatitis C virus	3/50 (5.9)	0 (0)	
Alcohol	1/50 (2.0)	2/26 (7.7)	
Others	2/50 (4.0)	0 (0)	
Child-Pugh class			< 0.001
A	103 (85.8)	77 (100)	
B	16 (13.3)	0 (0)	
C	1 (0.8)	0 (0)	
Tumor markers			
AFP†	8.3 (3.2, 138.3)	17.2 (4.5, 238.6)	0.147
> 147 ng/mL	28 (23.3)	25 (32.5)	0.156
PIVKA II†	45 (20.0, 459.8)	91 (25.8, 309.8)	0.383
> 219 mAU/mL	29 (24.2)	14 (18.2)	0.321
Tumor size, cm†	3.5 (2.8, 5.7)	3.5 (2.5, 6.1)	0.707
Pathologic diagnosis			
HCC	77 (64.2)	65 (84.4)	0.002
Edmondson grade			
I or II	24 (31.2)	27 (35.1)	0.570
III or IV	53 (68.8)	40 (51.9)	0.017
Non-HCC malignancy			
cHCC-CCA	12 (10.0)	5 (6.5)	0.395
CCA	31 (25.8)	6 (7.8)	0.002
NEC	0 (0)	1 (1.3)	0.212
Pathologic MVI	51 (42.5)	39 (50.6)	0.267
Pathologic satellite nodule	18 (15.0)	12 (15.6)	0.909
Type of liver surgery			
Anatomic resection	102 (85.0)	56 (72.7)	0.035
Non-anatomic resection	13 (10.8)	21 (27.3)	0.002
Liver transplantation	5 (4.2)	0 (0)	0.069
Positive resection margin	10 (8.3)	5 (6.5)	0.643
Follow-up data			
Follow-up period, month†	49 (17.5, 76.8)	57 (24.0, 92.0)	0.070
Recurrence	69 (57.5)	45 (58.4)	0.901
Death	31 (25.8)	20 (26.0)	0.987
RFS, month†	23.9 (6.5, 60.4)	41.5 (7.5, 66.5)	0.188
OS, month†	50.2 (18.2, 76.4)	56 (26.6, 91.5)	0.123

Unless otherwise indicated, data are numbers with percentages in parentheses. *Data are average with standard deviation in parentheses, †Data are median with interquartile range in parentheses. AFP = alpha-fetoprotein, CCA = cholangiocarcinoma, cHCC-CCA = combined HCC-CCA, HCC = hepatocellular carcinoma, MVI = microvascular invasion, NAFLD = non-alcoholic fatty liver disease, NEC = neuroendocrine carcinoma, OS = overall survival, PIVKA II = protein induced by vitamin K absence or antagonist II, RFS = recurrence-free survival

https://doi.org/10.3348/kjr.2022.0560

lesions. Rim APHE was the most common targetoid feature in both cohorts (96.7% vs. 100%). The inter-reader agreement for the MRI findings was good to excellent (κ, 0.61–0.99) (Table 2, Supplementary Table 3). For three novel prognostic features (thin- or thick-rim APHE, vascular involvement other than TIV, and HBP hypointense nodule without APHE), the overall inter-reader agreement was likewise good to excellent (κ, 0.71–0.80). When compared by experience levels, more experienced readers showed slightly higher agreement (κ, 0.87–0.96) than the less experienced reader (κ, 0.56–0.91), more so in identifying HBP hypointense nodules without APHE (0.56 to 0.64 vs. 0.77 to 0.93) (Supplementary Table 4).

Clinical and Radiologic Predictors for RFS and OS in Targetoid Lesions

In the development cohort, during the median follow-up period of 49 months (range, 1.3–126.6; and interquartile range, 17.5–76.8 months), 69 patients (57.5%) had recurrences, and 31 patients (25.8%) died. Tables 3 and 4 list the results of univariable and multivariable Cox analyses for RFS and OS, respectively. The cumulative incidences of recurrence were 35.7%, 44.1%, and 56.7% at one, two, and five years, respectively. In RFS model 1, which excluded HBP imaging features, tumor size of ≥ 2 cm (hazard ratio [HR]: 3.42; 95% confidence interval [CI]: 1.16, 10.05 for 2–5 cm; HR: 6.47; 95% CI: 2.09, 20.01 for > 5 cm) and thin-rim APHE (HR: 2.98; 95% CI: 1.66, 5.36) were effective predictors of recurrence. When all features were accounted for in RFS model 2, tumor size of > 5 cm (HR: 3.48; 95% CI: 1.07, 11.35), TIV (HR: 2.86; 95% CI: 1.26, 6.48), and HBP hypointense nodules without APHE (HR: 4.03; 95% CI: 2.03, 8.01) predicted recurrence (Fig. 4).

The one-, two-, and five-year OS rates were 91.1%, 83.6%, and 73.0%, respectively. Multivariable analysis revealed that tumor size of > 5 cm (HR: 2.94; 95% CI: 1.33, 6.53), thin-rim APHE (HR: 4.48; 95% CI: 1.99, 10.08), TIV (HR: 3.89; 95% CI: 1.25, 12.11), and vascular involvement other than TIV (HR: 3.31; 95% CI: 1.31, 8.36) were predictors of mortality.

In the subgroup analysis by pathological diagnosis, RFS was comparable across all pathological diagnoses, but OS was significantly lower in CCA than in HCC (p = 0.022) (Supplementary Fig. 1).

Table 2. Gadoxetic Acid-Enhanced MRI Findings in Development Cohort

	Inter-Reader Agreement (κ)*	Patients (n = 120)†
Targetoid features		
Rim APHE	0.75 (0.66, 0.84)	
Thin rim		42 (35.0)
Thick rim		74 (61.7)
Peripheral washout	0.73 (0.63, 0.84)	45 (37.5)
Delayed central enhancement	0.81 (0.71, 0.91)	47 (39.2)
Targetoid diffusion restriction	0.78 (0.67, 0.88)	58 (48.3)
Targetoid TP or HBP appearance	0.85 (0.75, 0.96)	57 (47.5)
Corona enhancement	0.72 (0.62, 0.82)	52 (43.3)
Capsule	0.80 (0.70, 0.90)	27 (22.5)
Intralesional fat	0.84 (0.74, 0.95)	21 (17.5)
Peritumoral bile duct dilatation	0.94 (0.84, 1.00)	21 (17.5)
Nonsmooth tumor margin	0.85 (0.75, 0.96)	90 (75.0)
TIV	0.94 (0.84, 1.00)	11 (9.2)
Vascular involvement other than TIV	0.80 (0.70, 0.91)	57 (47.5)
Peritumoral hypointensity on HBP	0.88 (0.77, 0.98)	52 (43.3)
HBP hypointense nodule without APHE	0.71 (0.61, 0.82)	38 (31.7)

*Numbers in parentheses are 95% confidence intervals, †Data are numbers with percentages in parentheses, based on the consensus assessment. APHE = arterial phase hyperenhancement, HBP = hepatobiliary phase, TIV = tumor in vein, TP = transitional phase

Stratification of RFS and OS according to Risk Score

For RFS models, the risk scores ranged from 0 to 3. The risk score showed good discriminatory performance, with a C-index of 0.67 (95% CI: 0.60, 0.75), and 0.62 (95% CI: 0.54, 0.70) for RFS models 1 and 2, respectively, in the validation cohort. The AUCs at one-, two-, and five years for RFS model 1 were 0.69 (95% CI: 0.54, 0.84), 0.72 (95% CI: 0.57, 0.87), and 0.69 (95% CI: 0.54, 0.85), respectively, and those for RFS model 2 were 0.68 (95% CI: 0.57, 0.80), 0.67 (95% CI: 0.56, 0.77), and 0.58 (95% CI: 0.46, 0.70), respectively, in the validation cohort (Supplementary Table 5). The models showed comparable performances (all p > 0.05).

The risk score for OS ranged from 0 to 3 and similarly showed good discriminatory performance with a C-index of 0.76 (95% CI: 0.65, 0.86), and the AUCs at one-, two-, and five-year were 0.76 (95% CI: 0.65, 0.86), 0.72 (95% CI: 0.54, 0.89), and 0.80 (95% CI: 0.67, 0.92), respectively, in the validation cohort (Supplementary Table 5).

The patients were stratified into three risk groups by cutoff scores corresponding to two-year RFS and OS

https://doi.org/10.3348/kjr.2022.0560

Table 3. Univariable and Multivariable Cox Analyses of RFS in the Development Cohort

	Univariable Analysis			Multivariable Analysis for RFS Model 1					Multivariable Analysis for RFS Model 2				
	HR	95% CI	*P*	β	HR	95% CI	*P*	Risk Score	β	HR	95% CI	*P*	Risk Score
Age (per year)	0.99	0.97, 1.02	0.649										
Male [female]	1.02	0.61, 1.71	0.931										
Hepatitis B [non-hepatitis B]	0.80	0.47, 1.31	0.417										
AFP (> 147 ng/mL)	1.74	1.03, 2.95	0.039	0.04	1.04	0.46, 2.34	0.925		-0.33	0.72	0.35, 1.50	0.383	
PIVKA II (> 219 mAU/mL)	2.15	1.24, 3.75	0.007	0.36	1.43	0.75, 2.72	0.273		0.20	1.22	0.54, 2.78	0.636	
Tumor size, cm													
< 2		Reference											
2–5	1.66	0.70, 3.94	0.247	1.23	3.42	1.16, 10.05	0.026	1	0.98	2.65	0.89, 7.90	0.079	
> 5	3.15	1.29, 7.69	0.012	1.87	6.47	2.09, 20.01	0.001	2	1.25	3.48	1.07, 11.35	0.038	1
Child-Pugh B/C [A]	1.17	0.78, 2.75	0.230										
Pathologic features													
Non-HCC malignancy [HCC]	1.23	0.76, 2.01	0.400										
Cirrhosis (F4) [F0–F3]	0.78	0.48, 1.27	0.319										
Pathologic MVI	1.69	1.05, 2.73	0.031	0.02	1.02	0.50, 2.07	0.954		-0.15	0.86	0.43, 1.73	0.670	
Pathologic satellite nodule	2.19	1.22, 3.95	0.009	0.61	1.84	0.91, 3.71	0.091		0.35	1.42	0.69, 2.92	0.339	
Radiologic features													
Thin rim APHE [thick rim]	2.02	1.24, 3.29	0.005	1.09	2.98	1.66, 5.36	< 0.001	1	0.63	1.87	0.99, 3.55	0.056	
Peripheral washout													
Delayed central enhancement	1.58	0.98, 2.55	0.062	0.05	1.05	0.53, 2.10	0.889		0.22	1.25	0.64, 2.45	0.514	
Targetoid diffusion restriction	1.29	0.81, 2.08	0.286										
Targetoid TP or HBP appearance	0.92	0.57, 1.48	0.740										
Corona enhancement	1.45	0.90, 2.32	0.128										
Capsule	1.14	0.66, 1.97	0.648										
Intralesional fat	0.99	0.54, 1.82	0.979										
Peritumoral bile duct dilatation	1.88	1.08, 3.26	0.025	-0.48	0.62	0.28, 1.35	0.228		-0.37	0.69	0.31, 1.58	0.383	
Nonsmooth tumor margin	0.92	0.53, 1.59	0.756										
TIV	2.11	1.00, 4.43	0.049	0.74	2.09	0.97, 4.53	0.061		1.05	2.86	1.26, 6.48	0.012	1
Vascular involvement other than TIV	1.30	0.81, 2.11	0.281										
Peritumoral hypointensity on HBP	1.72	1.07, 2.76	0.026	…	…	…	…		0.31	1.36	0.64, 2.89	0.426	
HBP hypointense nodule without APHE	4.31	2.59, 7.15	< 0.001	…	…	…	…		1.39	4.03	2.03, 8.01	< 0.001	1

Square brackets indicate reference categories. AFP = alpha-fetoprotein, APHE = arterial phase hyperenhancement, CI = confidence interval, HBP = hepatobiliary phase, HCC = hepatocellular carcinoma, HR = hazard ratio, MVI = microvascular invasion, PIVKA II = protein induced by vitamin K absence or antagonist II, RFS = recurrence-free survival, TIV = tumor in vein, TP = transitional phase

KJR Korean Journal of Radiology

Table 4. Univariable and Multivariable Cox Analyses of OS in the Development Cohort

	Univariable Analysis			Multivariable Analysis for OS Model				
	HR	95% CI	*P*	β	HR	95% CI	*P*	Risk Score
Age (per year)	1.02	0.98, 1.06	0.406					
Male [female]	1.11	0.53, 2.35	0.783					
Hepatitis B [non-hepatitis B]	0.52	0.25, 1.10	0.088	0.17	1.19	0.45, 3.17	0.727	
AFP (> 147 ng/mL)†	1.58	0.72, 3.46	0.250	-0.32†	0.73	0.28, 1.93	0.524	
PIVKA II (> 219 mAU/mL)	1.61	0.74, 3.54	0.232					
Tumor size, cm								
2–5 [< 2]	3.54	0.47, 26.81	0.221					
> 5 [< 2]	9.16	1.21, 69.46	0.032	1.08	2.94‡	1.33, 6.53	0.008	1
Child-Pugh B/C [A]	1.52	0.62, 3.71	0.361					
Pathologic features								
Non-HCC malignancy [HCC]	2.17	1.06, 4.42	0.034	0.36	1.44	0.52, 3.98	0.488	
Cirrhosis (F4) [F0–F3]	0.78	0.37, 1.62	0.497					
Pathologic MVI	2.14	1.05, 4.39	0.037	0.19	1.21	0.43, 3.43	0.724	
Pathologic satellite nodule	3.50	1.60, 7.66	0.002	0.57	1.77	0.75, 4.16	0.193	
Radiologic features								
Thin rim APHE [thick rim]	3.45	1.63, 7.31	0.001	1.50	4.48	1.99, 10.08	< 0.001	1
Delayed central enhancement	2.18	1.07, 4.45	0.032	0.25	1.29	0.51, 3.25	0.592	
Targetoid diffusion restriction	1.49	0.73, 3.02	0.272					
Targetoid TP or HBP appearance	1.54	0.76, 3.13	0.232					
Corona enhancement	1.79	0.88, 3.64	0.107					
Capsule	0.83	0.36, 1.93	0.664					
Intralesional fat	0.47	0.14, 1.54	0.468					
Peritumoral bile duct dilatation	3.49	1.69, 7.21	0.001	0.68	1.97	0.80, 4.86	0.142	
Nonsmooth tumor margin	1.09	0.47, 2.53	0.845					
TIV*	3.46	1.41, 8.51	0.007	1.36	3.89	1.25, 12.11	0.019	1*
Vascular involvement other than TIV*	2.19	1.08, 4.44	0.030	1.20	3.31	1.31, 8.36	0.011	1*
Peritumoral hypointensity on HBP	1.99	0.97, 4.07	0.059	-0.71	0.49	0.17, 1.40	0.183	
HBP hypointense nodule without APHE	2.22	1.08, 4.57	0.031	0.44	1.55	0.57, 4.24	0.394	

Square brackets indicate reference categories. *Mutually exclusive by definition; thus, the highest total risk score was 3, †Included in the multivariable analysis due to known substantial correlation with survival [41], ‡Compared to tumor size ≤ 5 cm. AFP = alpha-fetoprotein, APHE = arterial phase hyperenhancement, CI = confidence interval, HBP = hepatobiliary phase, HCC = hepatocellular carcinoma, HR = hazard ratio, MVI = microvascular invasion, OS = overall survival, PIVKA II = protein induced by vitamin K absence or antagonist II, TIV = tumor in vein, TP = transitional phase

probabilities of approximately 70% and 30%, respectively (Supplementary Table 6). The Kaplan–Meier curves and log-rank test demonstrated that risk groups in RFS and OS models had distinct matching outcomes in both cohorts (RFS models, all $p \leq 0.011$; OS model, all $p \leq 0.033$, in the validation cohort) (Fig. 5). In the development cohort, the estimated one-year RFS rates in the favorable-, intermediate-, and poor-risk groups were 79.1%, 50.2%, and 33.3% for RFS model 1, respectively, and 78.4%, 51.4%, and 0%, respectively, for RFS model 2. The estimated five-year OS rates in the favorable-, intermediate-, and poor-risk groups were 82.6%, 62.0%, and 25.0%, respectively.

Relationship between Radiologic Findings and Pathologic Results

The correlation between the pathological results and radiologic findings was explored (Supplementary Table 7). HCCs were associated with thick-rim APHE (odds ratio [OR], 6.7), absence of delayed central enhancement (OR, 3.5), no targetoid appearance on DWI/TP/HBP (OR, 2.7–5.1), and presence of capsule (OR, 9.9) ($p < 0.01$). MVI was associated with vascular involvement other than TIV (OR, 2.2) and hypointense nodules without APHE (OR, 3.1) ($p < 0.05$).

https://doi.org/10.3348/kjr.2022.0560

Korean Journal of Radiology
KJR

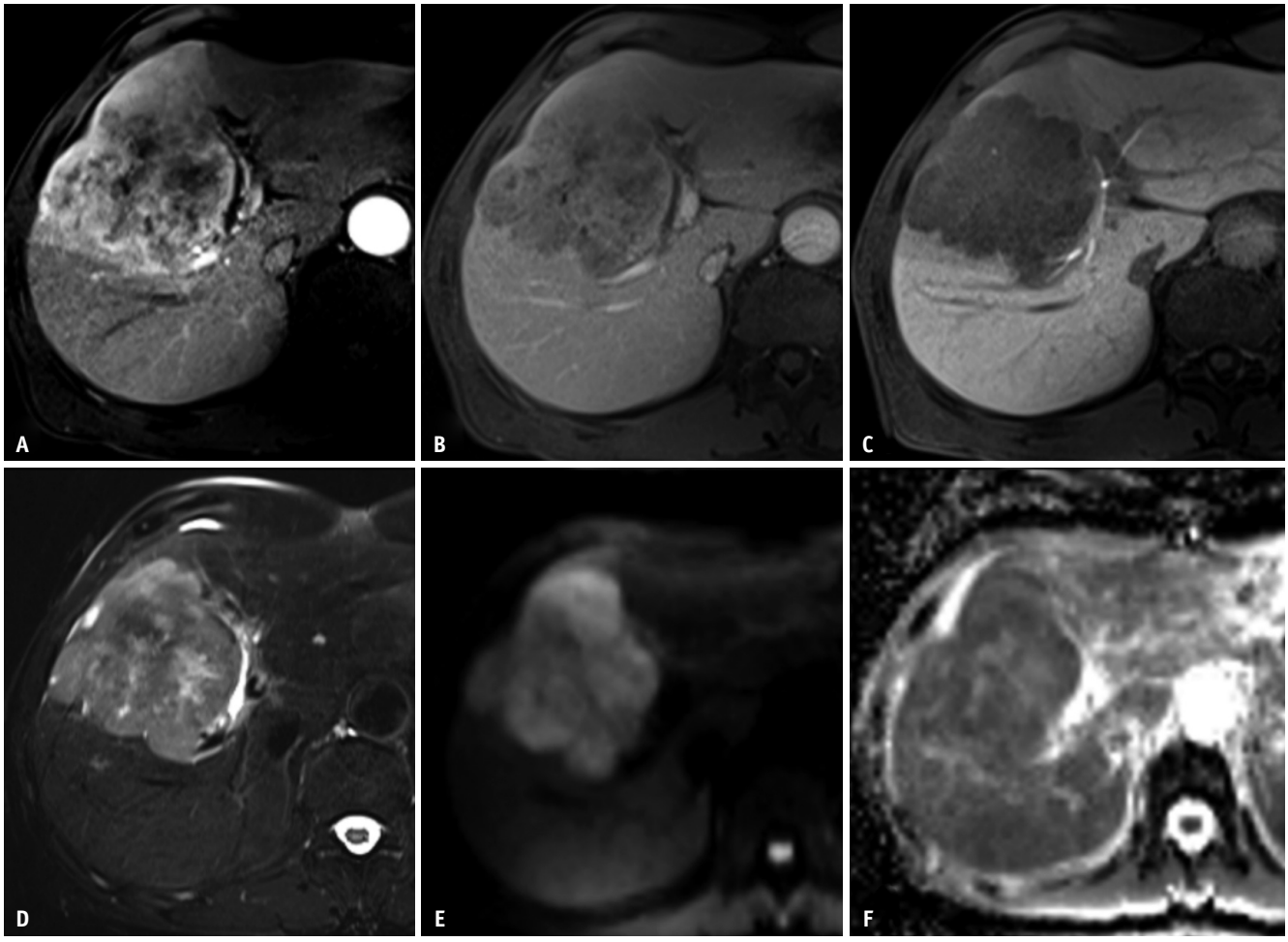

Fig. 4. Preoperative gadoxetic acid-enhanced MR images of a 61-year-old male chronic hepatitis B patient.
A-C. There is an 8.4-cm mass **(A)** with thick arterial rim enhancement in S4 and S8 of the liver, with **(B)** portal venous phase washout and portal vein branch obliteration, and **(C)** peritumoral hypointensity on the hepatobiliary phase. **D-F.** The mass **(D)** shows a targetoid appearance on the T2-weighted image with **(E, F)** restricted diffusion. The patient belongs to the intermediate-risk group for recurrence and survival. A right hemihepatectomy was performed, and the pathologic report showed cholangiocarcinoma with microvascular invasion. The patient has been disease-free for six years.

DISCUSSION

Targetoid appearance in primary liver malignancies has been associated with poor surgical outcomes and aggressive histopathologic features [10,11,32]. However, further prognostic stratification within targetoid lesions has been neglected. We evaluated the factors associated with recurrence and survival after curative surgery for targetoid primary liver malignancy and developed risk stratification models. On multivariable analysis, tumor size of ≥ 2 cm, thin-rim APHE, hypointense HBP nodules without APHE, TIV, and vascular involvement other than TIV were independent predictors of recurrence and death. The integrated risk scores classified the patients into three distinct risk groups for recurrence and death. Our results may help preoperatively identify targetoid primary liver malignancies at risk of poor surgical outcomes, potentially modifying the extent of surgery or intensity of postoperative surveillance.

In our study, thin-rim APHE was associated with poorer RFS and OS than thick-rim APHE. Notably, thick-rim APHE was predominantly associated with HCC (74.0%; 57 of 77), whereas thin-rim APHE was observed in 65.1% (28 of 43) of non-HCC ($p < 0.001$). This suggests that the arterial enhancing area may reflect favorable pathologic features proportionally. Supporting this finding, a prior radiologic-pathologic correlation revealed that hypervascular tumors have a larger proportion of HCC in cHCC-CCA [33], and quantitative hypovascular areas are predictive of aggressive macrotrabecular-massive HCC [34]. Additionally, rim APHE of uneven thickness is significantly more common in cHCC-

 https://doi.org/10.3348/kjr.2022.0560

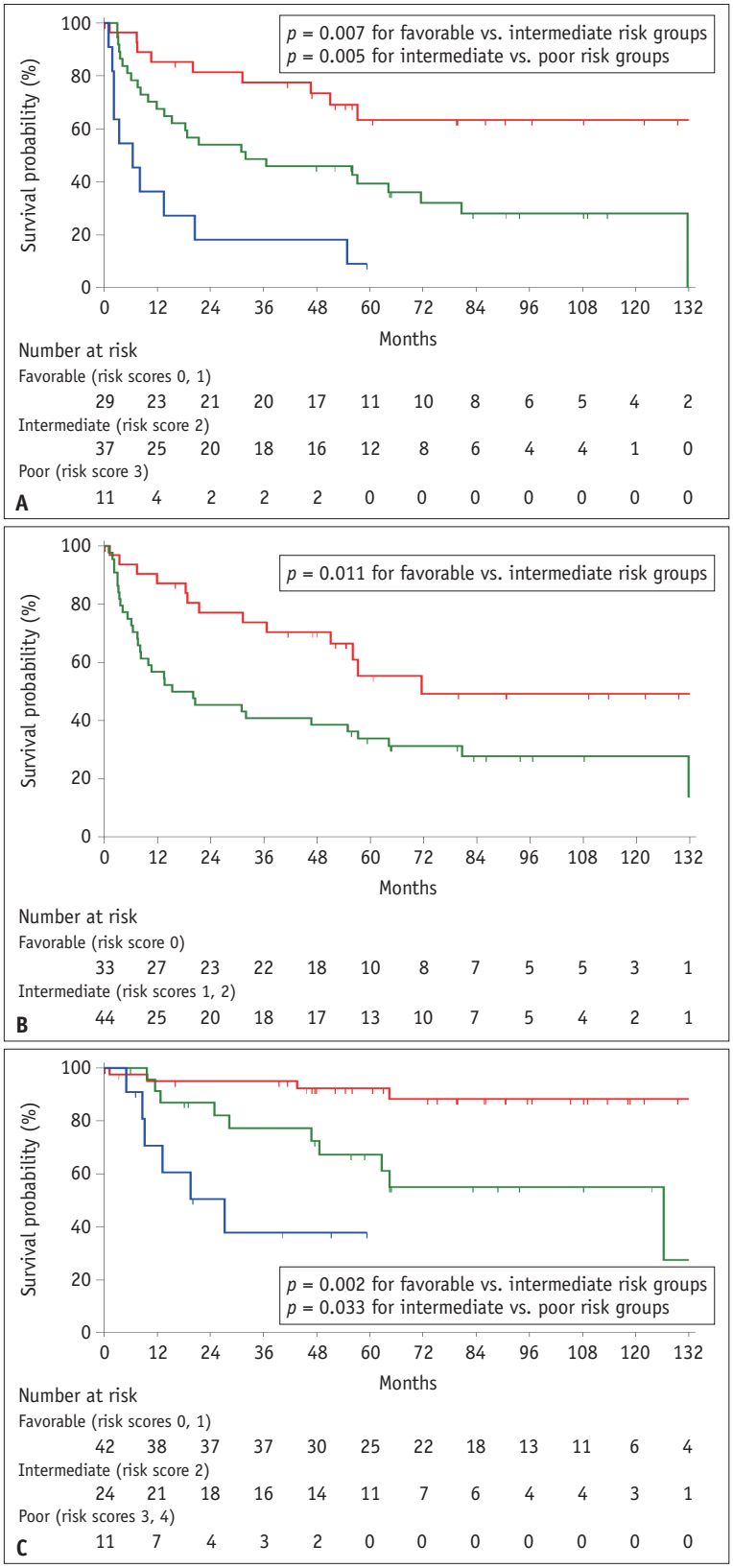

Fig. 5. RFS and OS for favorable-risk groups (red curves), intermediate-risk groups (green curves), and poor-risk groups (blue curves) in the validation cohort.
A-C. RFS model 1 **(A)**, RFS model 2 **(B)**, and OS model **(C)** show that RFS **(A, B)** and OS **(C)** differed significantly between score groups according to the log-rank test. OS = overall survival, RFS = recurrence-free survival

https://doi.org/10.3348/kjr.2022.0560

Korean Journal of Radiology
KJR

CCA than in CCA [7], suggesting a positive correlation between the arterial enhancing area and the HCC component. Although rim APHE is a known poor prognostic factor in primary liver malignancies [10,11,35,36], we showed that it might be further classified into reproducible patterns that significantly affect surgical outcomes, underlined by good inter-reader agreement and externally validated discriminatory power. However, given the reduced agreement with less experienced readers, acknowledging the proposed types of rim APHE and their prognostic impact is required for a consistent interpretation.

We developed two multivariable models for RFS that either included or excluded features only available on HBP to account for incidences where gadoxetic acid-enhanced MRI was unavailable or HBP images were suboptimal. Moreover, the risk scores from both models demonstrated comparable discriminatory performance, successfully addressing these challenges. Of the HBP features assessed, hypointense nodules without APHE were strong predictors of recurrence. Interestingly, for 28 HBP hypointense nodules in the recurrence group, the primary tumor was not only HCC (71.4%, 20 of 28) but also cHCC-CCA (17.9%, 5 of 28) and CCA (10.7%, 3 of 28). HBP hypointense nodules without APHE in HCC represent a spectrum of advanced HCC, early HCC, and high-grade dysplastic nodules [37,38], whereas they indicate intrahepatic metastasis in non-HCC malignancies [39]. Previous studies reported higher rates of early recurrence and shorter disease-free survival for HBP hypointense nodules without APHE [19,20] in HCC, consistent with our results. We assume that the spectrum of hepatocarcinogenesis or occult metastases without evident arterial enhancement is shown by our study's HBP hypointense nodule without APHE. The apparent disease recurrence most likely reduced RFS and OS. Although we could not reveal the histopathologic nature of these nodules, we have established grounds for a strong argument that in both HCC and non-HCC malignancies, HBP hypointense nodules left unresected are influential risk factors, warranting sensitive radiological detection and consideration for removal.

Other than TIV, vascular involvement was an independent predictor of death and related to pathologic MVI. Considering that the definition of MVI is “tumor emboli in the vascular endothelial space” [40], vascular involvement may be an indicator of MVI, but this relationship requires further validation. Aside from TIV, vascular involvement can be a useful prognostic factor in the context of relatively constant inter-reader agreement across reader experiences.

Our study had several limitations. First, it was a retrospective study with a selection bias. Second, patients with radiological macrovascular TIV (12.2%; 24 of 197) were included in the study, which could be viewed as a contraindication for surgery. However, the thrombi were located in the peripheral segmental branches and were deemed resectable by surgeons. With increasing surgical attempts to cure patients with TIV, our results reveal that TIV is a poor postoperative risk factor. Third, we did not perform a dedicated retrospective histopathologic review of cHCC-CCAs according to the latest 2019 World Health Organization classification, and some diagnoses may be outdated, although the number of cHCC-CCAs was small. Finally, because our study included patients with chronic liver disease that had heterogeneous etiologies, the proposed model may perform differently in populations exclusively with chronic hepatitis B or cirrhosis.

In conclusion, tumor size of ≥ 2 cm, thin-rim APHE, HBP hypointense nodules without APHE, and tumor vascular involvement were predictors of postoperative recurrence and death for targetoid primary liver malignancies in chronic liver disease, and derived and externally validated risk scores may help to predict postoperative RFS and OS in these patients.

Supplement

The Supplement is available with this article at https://doi.org/10.3348/kjr.2022.0560.

Availability of Data and Material

The datasets generated or analyzed during the study are available from the corresponding author on reasonable request.

Conflicts of Interest

The authors have no potential conflicts of interest to disclose.

Author Contributions

Conceptualization: Bohyun Kim, So Hyun Park. Data curation: Bohyun Kim, So Hyun Park, Subin Heo, Joon-Il Choi, Pil Soo Sung, Ho Joong Choi. Formal analysis: Jungbok Lee, Bohyun Kim, So Hyun Park. Funding acquisition: Bohyun Kim. Investigation: Bohyun Kim, So Hyun Park, Subin Heo. Methodology: Bohyun Kim, So Hyun

Park, Joon-Il Choi. Supervision: Bohyun Kim. Writing—original draft: So Hyun Park, Subin Heo. Writing—review & editing: Bohyun Kim, Subin Heo, Joon-Il Choi, Pil Soo Sung, Ho Joong Choi.

ORCID iDs
So Hyun Park
https://orcid.org/0000-0001-9935-2863
Subin Heo
https://orcid.org/0000-0002-4700-1014
Bohyun Kim
https://orcid.org/0000-0003-1157-415X
Jungbok Lee
https://orcid.org/0000-0002-1420-9484
Ho Joong Choi
https://orcid.org/0000-0002-0862-098X
Pil Soo Sung
https://orcid.org/0000-0002-5780-9607
Joon-Il Choi
https://orcid.org/0000-0003-0018-8712

Funding Statement
This study was supported by the National Research Foundation of Korea (NRF) grant funded by the Ministry of Science and ICT, Korea (NRF-2022R1F1A1071409).

REFERENCES

1. Llovet JM, Kelley RK, Villanueva A, Singal AG, Pikarsky E, Roayaie S, et al. Hepatocellular carcinoma. *Nat Rev Dis Primers* 2021;7:6
2. American College of Radiology. LI-RADS® CT/MRI. acr.org Web site. https://www.acr.org/Clinical-Resources/Reporting-and-Data-Systems/LI-RADS/LI-RADS-CT-MRI-v2018. Accessed February 27, 2021
3. Marrero JA, Kulik LM, Sirlin CB, Zhu AX, Finn RS, Abecassis MM, et al. Diagnosis, staging, and management of hepatocellular carcinoma: 2018 practice guidance by the American Association for the study of liver diseases. *Hepatology* 2018;68:723-750
4. European Association for the Study of the Liver. EASL clinical practice guidelines: management of hepatocellular carcinoma. *J Hepatol* 2018;69:182-236
5. Kim DH, Choi SH, Park SH, Kim KW, Byun JH, Kim SY, et al. Liver imaging reporting and data system category M: a systematic review and meta-analysis. *Liver Int* 2020;40:1477-1487
6. Heimbach JK, Kulik LM, Finn RS, Sirlin CB, Abecassis MM, Roberts LR, et al. AASLD guidelines for the treatment of hepatocellular carcinoma. *Hepatology* 2018;67:358-380
7. Kim SS, Lee S, Choi JY, Lim JS, Park MS, Kim MJ. Diagnostic performance of the LR-M criteria and spectrum of LI-RADS imaging features among primary hepatic carcinomas. *Abdom Radiol (NY)* 2020;45:3743-3754
8. Sammon J, Fischer S, Menezes R, Hosseini-Nik H, Lewis S, Taouli B, et al. MRI features of combined hepatocellular-cholangiocarcinoma versus mass forming intrahepatic cholangiocarcinoma. *Cancer Imaging* 2018;18:8
9. Park HJ, Kim YK, Cha DI, Ko SE, Kim S, Lee ES, et al. Targetoid hepatic observations on gadoxetic acid-enhanced MRI using LI-RADS version 2018: emphasis on hepatocellular carcinomas assigned to the LR-M category. *Clin Radiol* 2020;75:478.e13-478.e23
10. Choi SH, Lee SS, Park SH, Kim KM, Yu E, Park Y, et al. LI-RADS classification and prognosis of primary liver cancers at gadoxetic acid-enhanced MRI. *Radiology* 2019;290:388-397
11. An C, Kim DW, Park YN, Chung YE, Rhee H, Kim MJ. Single hepatocellular carcinoma: preoperative MR imaging to predict early recurrence after curative resection. *Radiology* 2015;276:433-443
12. An C, Park S, Chung YE, Kim DY, Kim SS, Kim MJ, et al. Curative resection of single primary hepatic malignancy: liver imaging reporting and data system category LR-M portends a worse prognosis. *AJR Am J Roentgenol* 2017;209:576-583
13. Jeon SK, Joo I, Lee DH, Lee SM, Kang HJ, Lee KB, et al. Combined hepatocellular cholangiocarcinoma: LI-RADS v2017 categorisation for differential diagnosis and prognostication on gadoxetic acid-enhanced MR imaging. *Eur Radiol* 2019;29:373-382
14. Shin J, Lee S, Kim SS, Chung YE, Choi JY, Park MS, et al. Characteristics and early recurrence of hepatocellular carcinomas categorized as LR-M: comparison with those categorized as LR-4 or 5. *J Magn Reson Imaging* 2021;54:1446-1454
15. Ariizumi S, Kitagawa K, Kotera Y, Takahashi Y, Katagiri S, Kuwatsuru R, et al. A non-smooth tumor margin in the hepatobiliary phase of gadoxetic acid disodium (Gd-EOB-DTPA)-enhanced magnetic resonance imaging predicts microscopic portal vein invasion, intrahepatic metastasis, and early recurrence after hepatectomy in patients with hepatocellular carcinoma. *J Hepatobiliary Pancreat Sci* 2011;18:575-585
16. Cho ES, Choi JY. MRI features of hepatocellular carcinoma related to biologic behavior. *Korean J Radiol* 2015;16:449-464
17. Sakon M, Nagano H, Nakamori S, Dono K, Umeshita K, Murakami T, et al. Intrahepatic recurrences of hepatocellular carcinoma after hepatectomy: analysis based on tumor hemodynamics. *Arch Surg* 2002;137:94-99
18. Kim KA, Kim MJ, Jeon HM, Kim KS, Choi JS, Ahn SH, et al. Prediction of microvascular invasion of hepatocellular carcinoma: usefulness of peritumoral hypointensity seen on gadoxetate disodium-enhanced hepatobiliary phase images. *J Magn Reson Imaging* 2012;35:629-634
19. Toyoda H, Kumada T, Tada T, Niinomi T, Ito T, Sone Y, et al.

Non-hypervascular hypointense nodules detected by Gd-EOB-DTPA-enhanced MRI are a risk factor for recurrence of HCC after hepatectomy. *J Hepatol* 2013;58:1174-1180
20. Kim DK, An C, Chung YE, Choi JY, Lim JS, Park MS, et al. Hepatobiliary versus extracellular MRI contrast agents in hepatocellular carcinoma detection: hepatobiliary phase features in relation to disease-free survival. *Radiology* 2019;293:594-604
21. Bosman FT, Carneiro F, Hruban RH, Theise ND. *WHO classification of tumours of the digestive system*. Geneva: World Health Organization, 2010
22. Fowler KJ, Potretzke TA, Hope TA, Costa EA, Wilson SR. LI-RADS M (LR-M): definite or probable malignancy, not specific for hepatocellular carcinoma. *Abdom Radiol (NY)* 2018;43:149-157
23. Min JH, Kim JM, Kim YK, Kim H, Choi GS, Kang TW, et al. A modified LI-RADS: targetoid tumors with enhancing capsule can be diagnosed as HCC instead of LR-M lesions. *Eur Radiol* 2022;32:912-922
24. Cannella R, Fraum TJ, Ludwig DR, Borhani AA, Tsung A, Furlan A, et al. Targetoid appearance on T2-weighted imaging and signs of tumor vascular involvement: diagnostic value for differentiating HCC from other primary liver carcinomas. *Eur Radiol* 2021;31:6868-6878
25. Motosugi U, Murakami T, Lee JM, Fowler KJ, Heiken JP, Sirlin CB; LI-RADS HBA Working Group. Recommendation for terminology: nodules without arterial phase hyperenhancement and with hepatobiliary phase hypointensity in chronic liver disease. *J Magn Reson Imaging* 2018;48:1169-1171
26. Bae JS, Lee JM, Yoon JH, Jang S, Chung JW, Lee KB, et al. How to best detect portal vein tumor thrombosis in patients with hepatocellular carcinoma meeting the Milan criteria: gadoxetic acid-enhanced MRI versus contrast-enhanced CT. *Liver Cancer* 2020;9:293-307
27. Punt CJ, Buyse M, Köhne CH, Hohenberger P, Labianca R, Schmoll HJ, et al. Endpoints in adjuvant treatment trials: a systematic review of the literature in colon cancer and proposed definitions for future trials. *J Natl Cancer Inst* 2007;99:998-1003
28. Llovet JM, Di Bisceglie AM, Bruix J, Kramer BS, Lencioni R, Zhu AX, et al. Design and endpoints of clinical trials in hepatocellular carcinoma. *J Natl Cancer Inst* 2008;100:698-711
29. Liu Y, Yang T, Wei YW. What is the difference between overall survival, recurrence-free survival and time-to-recurrence? *Br J Surg* 2020;107:e634
30. Yang H, Bae SH, Nam H, Lee HL, Lee SW, Yoo SH, et al. A risk prediction model for hepatocellular carcinoma after hepatitis B surface antigen seroclearance. *J Hepatol* 2022;77:632-641
31. Park SY, Park JE, Kim H, Park SH. Review of statistical methods for evaluating the performance of survival or other time-to-event prediction models (from conventional to deep learning approaches). *Korean J Radiol* 2021;22:1697-1707
32. Rhee H, An C, Kim HY, Yoo JE, Park YN, Kim MJ. Hepatocellular carcinoma with irregular rim-like arterial phase hyperenhancement: more aggressive pathologic features. *Liver Cancer* 2019;8:24-40
33. Park SH, Lee SS, Yu E, Kang HJ, Park Y, Kim SY, et al. Combined hepatocellular-cholangiocarcinoma: gadoxetic acid-enhanced MRI findings correlated with pathologic features and prognosis. *J Magn Reson Imaging* 2017;46:267-280
34. Rhee H, Cho ES, Nahm JH, Jang M, Chung YE, Baek SE, et al. Gadoxetic acid-enhanced MRI of macrotrabecular-massive hepatocellular carcinoma and its prognostic implications. *J Hepatol* 2021;74:109-121
35. Kim B, Won JH, Kim J, Kwon Y, Cho HJ, Huh J, et al. Hepatic arterial infusion chemotherapy for advanced hepatocellular carcinoma: radiologic and clinical factors predictive of survival. *AJR Am J Roentgenol* 2021;216:1566-1573
36. Min JH, Kim YK, Choi SY, Kang TW, Lee SJ, Kim JM, et al. Intrahepatic mass-forming cholangiocarcinoma: arterial enhancement patterns at MRI and prognosis. *Radiology* 2019;290:691-699
37. Joo I, Kim SY, Kang TW, Kim YK, Park BJ, Lee YJ, et al. Radiologic-pathologic correlation of hepatobiliary phase hypointense nodules without arterial phase hyperenhancement at gadoxetic acid-enhanced MRI: a multicenter study. *Radiology* 2020;296:335-345
38. Hyodo T, Murakami T, Imai Y, Okada M, Hori M, Kagawa Y, et al. Hypovascular nodules in patients with chronic liver disease: risk factors for development of hypervascular hepatocellular carcinoma. *Radiology* 2013;266:480-490
39. Kang Y, Lee JM, Kim SH, Han JK, Choi BI. Intrahepatic mass-forming cholangiocarcinoma: enhancement patterns on gadoxetic acid-enhanced MR images. *Radiology* 2012;264:751-760
40. Rodríguez-Perálvarez M, Luong TV, Andreana L, Meyer T, Dhillon AP, Burroughs AK. A systematic review of microvascular invasion in hepatocellular carcinoma: diagnostic and prognostic variability. *Ann Surg Oncol* 2013;20:325-339
41. Bai DS, Zhang C, Chen P, Jin SJ, Jiang GQ. The prognostic correlation of AFP level at diagnosis with pathological grade, progression, and survival of patients with hepatocellular carcinoma. *Sci Rep* 2017;7:12870

 https://doi.org/10.3348/kjr.2022.0560